

Single Mechanosensitive and Ca²⁺-Sensitive Channel Currents Recorded from Mouse and Human Embryonic Stem Cells

Bernat Soria · Sergio Navas · Abdelkrim Hmadcha · Owen P. Hamill

Received: 12 October 2012 / Accepted: 4 November 2012 / Published online: 28 November 2012
© Springer Science+Business Media New York 2012

Abstract Cell-attached and inside-out patch clamp recording was used to compare the functional expression of membrane ion channels in mouse and human embryonic stem cells (ESCs). Both ESCs express mechanosensitive Ca²⁺ permeant cation channels (MscCa) and large conductance (200 pS) Ca²⁺-sensitive K⁺ (BK_{Ca2+}) channels but with markedly different patch densities. MscCa is expressed at higher density in mESCs compared with hESCs (70 % vs. 3 % of patches), whereas the BK_{Ca2+} channel is more highly expressed in hESCs compared with mESCs (~50 % vs. 1 % of patches). ESCs of both species express a smaller conductance (25 pS) nonselective cation channel that is activated upon inside-out patch formation but is neither mechanosensitive nor strictly Ca²⁺-dependent. The finding that mouse and human ESCs express different channels that sense membrane tension and intracellular [Ca²⁺] may contribute to their different patterns of growth and differentiation in response to mechanical and chemical cues.

Keywords Calcium sensitive channels · Embryonic stem cells · Mechanosensitive channels

Embryonic stem cells (ESCs) are self replicating, pluripotent cells with high differentiation potential (Smith 2001). Beginning in 1981, the isolation of mouse ESCs provided a powerful system for studying the regulatory mechanisms that underlie stem cell fate decisions during embryogenesis and also provided a key step in the generation of gene knockout mice (Evans and Kaufman 1981; Martin 1981; Thomas and Capecchi 1987; Bronson and Smithies 1994). In 1998, the isolation of human ESCs (Thomson et al. 1998) introduced the new discipline of regenerative medicine with its many possibilities for cell-based therapies to repair damaged tissues and treat degenerative diseases (Weissman 2005; Hmadcha et al. 2009). ESCs, like all nucleated cells, possess the genetic blueprint to reproduce the organism. However, ESCs are special in that under appropriate culture conditions they can either undergo unlimited self renewal or differentiate into the many different cell lineages that form the organism. As a consequence, there is great interest in identifying the critical signaling pathways and genetic networks that precipitate the choice between self renewal and differentiation. To date, most attention has focused on the role of soluble growth factors, cytokines and receptor-operated signaling pathways (Dreesen and Brivanlou 2007; Pera and Tam 2010). However, there is growing evidence that mechanical signals also play significant roles in ESC fate decisions (For reviews see Discher et al. 2009; Cohen and Chen 2008; Keung et al. 2010; D'Angelo et al. 2011; Lee et al. 2011; Sun et al. 2012). In particular, it has been shown that applying cyclic strain/stretch to mouse and human ESCs grown on elastic substrates can modify their fate decisions in different directions (Saha et al. 2006, 2008; Schmelter et al. 2006; Gwak et al. 2008; Shimizu et al. 2008; Heo and Lee 2011; Wan et al. 2011; Horiuchi et al. 2012; Teramura et al. 2012). Moreover, different strain/stretch-induced signaling pathways have been evoked to explain the different responses. In hESCs, stretch-induced release of

B. Soria · S. Navas · A. Hmadcha
Department of Stem Cells, Andalusian Center for Molecular
Biology and Regenerative Medicine (CABIMER), Seville, Spain

B. Soria · A. Hmadcha
CIBER de Diabetes y Enfermedades Metabólicas Asociadas
(CIBERDEM), Barcelona, Spain

O. P. Hamill (✉)
Department of Neuroscience and Cell Biology, University
of Texas Medical Branch, Galveston, TX, USA
e-mail: ohamill@utmb.edu

transforming growth factor-beta (TGF- β) and activation of TGF- β /activin/nodal inhibits differentiation and promote pluripotency (Saha et al. 2008), while in mESCs, stretch-induced generation of reactive oxygen species (ROS) and integrin-mediated PI3K-Akt signaling promotes differentiation (Schmelter et al. 2006; Heo and Lee 2011). Furthermore, although mouse and human ESCs share the same core transcription factor networks for self-renewal and pluripotency (Smith 2001; Rao 2004; Van Hoof et al. 2006; Koestenbauer et al. 2006) they also differ substantially in their growth requirements, and in particular, the mechanical interactions required to maintain their functions and viability (Ginis et al. 2004; Sato et al. 2003; Hayashi et al. 2007; Chowdhury et al. 2010; Xu et al. 2010). However, it remains to be determined whether they also differ in the molecules/mechanisms that directly sense and transduce mechanical cues into specific responses.

A major class of force-sensing molecule involves mechanosensitive (MS) membrane ion channels that are activated by membrane stretch (Patel et al. 2001; Hamill and Martinac 2001; Kung 2005; Gottlieb and Sachs 2012; Martinac 2012). MS channels are special in that they often incorporate both mechanosensor and mechanotransducer within the same molecule (Coste et al. 2010; Brohawn et al. 2012). In eukaryotic cells, two major functional subclasses of MS channels have been identified—MS Ca²⁺ permeant cation selective channels (MscCa)—and MS K⁺ selective channels (MscK). By transducing membrane stretch into changes in membrane potential and/or changes in intracellular [Ca²⁺], MS channel activity can influence a variety of downstream signaling pathways that regulate cell proliferation and differentiation (Machaca 2010; Kapur et al. 2007; Sundelacruz et al. 2009; Apati et al. 2012). Indeed, MscCa has been implicated in transducing the effects of cyclic stretch/strain applied to various adult cells (Naruse et al. 1998; Wang et al. 2001; Danciu et al. 2003; Ostrow et al. 2011). However, although previous studies of ESCs, using whole cell patch clamp and/or Ca²⁺ imaging techniques, have identified voltage-gated and receptor-gated channels (Yanagida et al. 2004; Wang et al. 2005; Jiang et al. 2010; Ng et al. 2010; Schwirtlich et al. 2010; Rodríguez-Gómez et al. 2012) there have been no reports regarding the expression of MS channels. To address this deficiency we use cell-attached and inside-out patch clamp recording to determine if mouse and human ESCs express MscCa and/or MscK.

Materials and Methods

Cell Culture

Cells of the mouse embryonic stem cell (mESC) line ES-D3 (CRL-1934, ATCC, Manassas, VA) were cultured on

gelatine-coated flasks with high glucose DMEM (Gibco/BRL, Life Technologies) containing 15 % fetal bovine serum (FBS; Hyclone, Logan, UT, USA), 1 % nonessential amino acids (Gibco/BRL), 0.1 % mM 2- β -mercaptoethanol (Gibco/BRL), 100 U/ml penicillin and 0.1 mg/ml streptomycin (Gibco/BRL), and leukemia inhibitor factor (LIF) 1,000 U/ml (Chemicon ESG1107). Confluent culture were trypsinized and replated every 5 days. Previous studies indicate that ES-D3 cells remain undifferentiated in the presence of LIF, and when injected into blastocysts efficiently form germ-line chimeras (Pease and Williams 1990).

The human embryonic stem cell (hESC) line (HS181) was derived in the Fertility Unit of Karolinska University Hospital, Huddinge at the Karolinska Institute after approval of a project entitled “Derivation and early differentiation and characterization of hESC lines” by the Karolinska Institute Research Ethics Board South, Drno 454/02. This line was derived from an embryo that could not be used for the infertility treatment of a couple. Both partners of the couple signed a consent form for donation of the embryo for derivation of a possible permanent stem cell line to be used in stem cell research. The HS181 line is included in the EU hESC registry (<http://www.hescereg.eu/>) and cultured as described by Hovatta et al. (2003).

Patch Clamp Methods

Standard cell-attached and inside-out patch configurations (Hamill et al. 1981; Hamill 2006) were used to record single channel currents from murine and human ESCs that were bathed in the standard bath solution (Kreb's) containing in mM: 150 NaCl, 2.5 KCl, 1 CaCl₂, 1 MgCl₂ and 10 Hepes (NaOH) at pH 7.4. Patch pipette electrodes were made from borosilicate glass capillaries with an outside diameter of 1.5 mm and an inside diameter of 0.86 mm (A-M Systems, Calsborg, WA, USA) pulled with a Sutter P-97 horizontal puller (Sutter Instruments, Novato, CA, USA) to have a final tip resistances of 5–10 mega Ohm. The pipettes were used immediately after pulling without heat polishing or coating the tip. The suction port of the pipette holder was connected via a valve arrangement to a manometer that allowed the application of defined positive and/or negative pulses to the pipette to obtain the seal and afterward mechanically stimulate the patch. To obtain the initial giga-seal a slight positive pressure of 5 mm Hg was applied as the pipette approached and touched the cell. Suction (5–10 mmHg) was then applied to initially form the seal while slowly hyperpolarizing the patch potential (i.e., by polarizing the pipette potential from 0 to ≥ 50 mV) to further increase the resistance of the seal. To form the inside-out patch configuration, the pipette was pulled away from the cell and then, if necessary, the tip rapidly passed

across the solution-air interface. In some cases, as judged by full amplitude unitary channel activity after the first step, the second step (i.e., tip through the solution-air interface) was deemed unnecessary. Membrane currents were measured with a patch-clamp amplifier (Axon 200B; Axon Instruments, Foster City, CA), sampled, and analyzed with a Digidata 1320A interface and a personal computer with Clampex and Clampfit software (version 9.0.1, Axon Instruments). All recordings were performed at room temperature (22–23 °C) on the stage of an inverted microscope. Several pipette solutions were used to record from cell-attached and inside-out patches. The most commonly used were 100 Na⁺/1 Ca²⁺ which contained (in mM): 100 NaCl, 1 CaCl₂ (NaOH), 5 Hepes (NaOH) at pH 7.4; 100 Na⁺/0 Ca²⁺ which contained 100 NaCl, 5 EGTA (NaOH), 5 Hepes (NaOH) at pH 7.4. The relatively hypotonic pipette solution improved sealing without altering the channel activities seen with more isotonic pipette solutions (i.e., 140 mM NaCl) and also allowed direct comparison between I–Vs measured in cell-attached patches on *Xenopus* oocytes and human prostate tumor cells (Maroto et al. 2005, 2012). To measure the ion conductance of the channels, 100 mM NaCl was replaced with, for monovalents, 100 mM TEACl, 100 mM KCl, or 100 mM CsCl, and for divalents by 70 mM BaCl₂ or 70 mM CaCl₂ (without EGTA). The membrane potential of ESCs was estimated to be approximately –15 mV (range –10 to –20 mV) based on the reversal potential of nonselective cation and K⁺ selective channels measured with “140 mM K⁺ pipette solutions.” To evaluate single channel current–voltage (I–V) relations, membrane potential was manually stepped in 10 mV increments from –120 to 60 mV. The patch membrane potential (V_{patch}) is described by the relation: $V_{\text{patch}} = V_{\text{cell}} - V_{\text{pipette}}$ where V_{cell} is the cell membrane potential and V_{pipette} is the potential imposed on the recording pipette. By convention, inward channel currents are shown as downward deflections.

Results

Cell-Attached Patch Recordings from Mouse Embryonic Stem Cells

Most cell-attached patches formed on mESCs (i.e., 125/185) were “quiet” and expressed no spontaneous single channel current activity at resting or hyperpolarized patch potentials. The remaining 1/3 of patches showed a low frequency of spontaneous unitary inward currents (3–4 pA at –100 mV). Furthermore, all 60 of the spontaneously active patches, as well as more than half of the quiet patches (i.e., 70/125) responded to suction pulses (10–40 mm Hg) with rapid activation of unitary inward

currents (3–4 pA at $V_{\text{patch}} -100$ mV) with an average of ~5 channels (range 1–10 channels) maximally activated in these patches. The other 30 % of patches (i.e., 55/185) failed to respond to even larger suction (100 mm Hg) indicating an absence of functional stretch-activated channels. In initial experiments, we also tested the effects of positive pressure stimulation. However, even small pressure pulses of 10–20 mm Hg caused large, noisy, and often irreversible, increases in current consistent with patch/seal disruption.

Figure 1a shows unitary inward MS currents activated by a suction pulse of 20 mm Hg and recorded at a patch potential of –100 mV. The single MS current events in this trace indicate multiple unitary conductance states with more frequent ~4 pA events, and less frequent ~3 pA events. After the pulse, a low frequency of even smaller (~0.5 pA) events was detected in the same patch. Figure 1b describes another patch that expressed spontaneous events preceding stimulation that had the same amplitude as the most common MS current event. Typically, the largest MS response was evoked by the first pulse and then faded with subsequent pulses (Fig. 1b). In the same patch, two notable kinetic features were evident—first, after a rapid rise to a peak the MS current rapidly declined toward baseline despite maintained suction—second, after the stimulus pulse the MS current showed a delayed turn-off. Not all MS currents in patches showed these kinetic features. For example, some patches showed sustained, rather than transient currents, and in other patches the current turned off with suction. The difference between transient and sustained currents may be related to mechanical fragility of the MS channel adaptation/inactivation mechanism and the mechanical effects of the initial suction necessary to achieve a tight seal with the membrane patch (Maroto et al. 2012).

Figure 2a shows cell-attached patch recordings of unitary MS currents activated by steady-state suction (~10 mm Hg) and measured at different membrane patch potentials. MS channels recorded at strongly hyperpolarized patch potentials (–120 mV) had a higher opening frequency and briefer open lifetime than channels measured at the most depolarized potential (80 mV). Similar voltage-dependent open channel kinetics have also been reported for MS cation channels recorded from *Xenopus* oocytes (Taglietti and Toselli 1988) and human prostate tumor cells (Maroto et al. 2012; cf. our Fig. 2a with Fig. 2A of Taglietti and Toselli 1988; and fig. 9A of Maroto et al. 2012). Selected traces from the same patch recording (Fig. 2a, –20 mV trace) also indicated smaller amplitude unitary events along side larger events (i.e., main state). But not all patches displayed the smaller events (~75 % of the main state). For example, in one of our most stable patch recordings in which 850 unitary events were examined, only the main conductance state

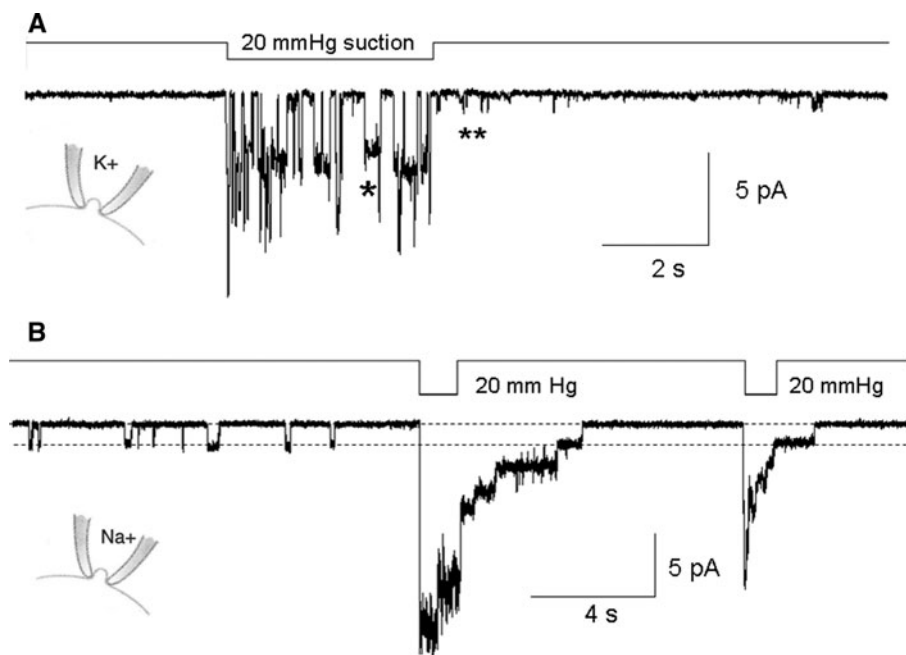


Fig. 1 Cell-attached patch recording from mouse ESCs. **a** Suction pulse activation of unitary inward currents. The *asterisk* designates a relatively smaller unitary current (~ 3 pA) compared with the more common events of ~ 4 pA. The *double asterisk* indicates the smaller events (~ 0.5 pA) that increase after the pulse. In this and subsequent figures, the *upper trace* represents the suction applied to the patch pipette and the *lower trace* represents the patch current. The recording was made with a 100 mM K^+ /0 mM Ca^{2+} pipette solution at a patch

potential of -100 mV. **b** Cell-attached patch recording from another mESC shows spontaneous unitary inward currents before applying suction to the patch that had the same amplitude as the unitary MS events resolved during the gradual MS current turn-off. Typically, the first pulse applied to a patch evoked the largest peak current with subsequent pulses evoking smaller currents. Recordings made with a 100 mM Na^+ /1 mM Ca^{2+} pipette solution at a patch potential of -50 mV

was detected (data not shown). This type of patch-to-patch variation at least supports the idea of heterogeneous and spatially separated MS channel types with different single channel conductance. However, evidence for the alternative possibility of a single channel switching between conductance states was also supported by current events in another patch described in Fig. 2b. In this case, at least three current levels (designated small, medium, and big) were seen, both as discrete events and also as transitions during a single event. Similar multiple conductance state behavior has been reported for MS cation channels in a variety of other cell types and both mechanisms have been evoked (Yamamoto and Suzuki 1996; Yao et al. 2001; Gil et al. 2001; Cho et al. 2006; Suchyna et al. 2004; Vasquez et al. 2012). In the most recent study, MS unitary current events were examined as a function of time during the recording, and were found to vary in a nonrandom manner between small and large amplitudes (Vasquez et al. 2012). On the basis of this result, it was concluded that the two amplitude events arise from the gating of a single channel molecule that may exist in either one of two distinct conductance states. For mESC patches, we could not record sufficient numbers of the S, M and B events (mainly as a result of stretch-induced run-down of activity) to carry out a similar analysis/distinction.

Conductance Properties of the MS Channels in Mouse Embryonic Stem Cells

With high Na^+ (100 mM) in the pipette solution, and recording at hyperpolarized patch potentials, suction pulses only activated inward currents (~ 40 patches) consistent with stretch-activated cation channels, but inconsistent with functional stretch-activated K^+ selective channels in mESCs. Replacement of the 100 mM NaCl in the pipette solution with 100 mM TEACl significantly reduced the size (by $>90\%$) of MS inward currents and shifted the reversal potential from ~ 0 to 30 mV without blocking outward currents measured at more depolarized potentials. This behavior is also consistent with cation channels (data not shown). MS channel currents measured with 100 mM KCl , 100 mM CsCl , 70 mM BaCl_2 or 70 mM CaCl_2 in the pipette solution indicated nonselective cation channels with significant conductance for both monovalent and divalent cations. Figure 3 shows MS currents measured with external Cs^+ (Fig. 3a) and Ca^{2+} (Fig. 3b). In the specific case of high external Ca^{2+} there was increased spontaneous MS channel openings and average channel open time was reduced (Fig. 3b). Figure 3c, d show current–voltage (I–V) relations from cell-attached patches comparing the main conductance of the MS channels for external K^+ versus

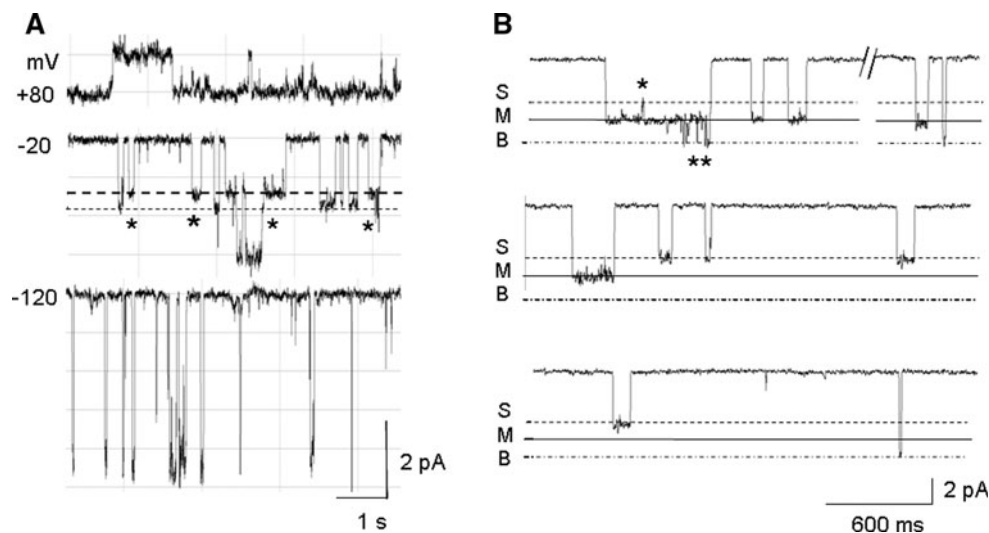


Fig. 2 MS channel properties measured on cell-attached patches on mESC. **a** A steady-state suction of ~ 10 mm Hg was applied to the patch to evoke a low frequency of unitary currents which were recorded at the designated patch potentials. The trace recorded at a patch potential of -20 mV indicated heterogeneities in the unitary inward currents with a predominant event of ~ 2 pA and a smaller current event of 1.5 pA. Recordings made with a 100 mM K⁺/5 mM EGTA pipette solution. **b** High-resolution single MS channel current recordings illustrating multiconductance state behavior. All current traces were recorded from the same mESC cell-attached patch held at

-120 mV with 100 mM KCl/5 mM EGTA pipette solution and a steady state suction of ~ 5 mm Hg applied to the patch. The *top current trace* shows a long open event in which the current switches between a Main, a Smaller (*asterisk*) and a Bigger (*double asterisk*) levels/states. The other currents (*far right*) included discrete M events and a B event within a selected segment of a different trace. The *middle trace* shows the initial M event that undergoes brief transition to S levels and subsequent discrete S state events. The *lower trace* shows a discrete S event and a brief discrete B event

Na⁺ (100 mM, Fig. 3c) and for Ba²⁺ versus Ca²⁺ (70 mM, Fig. 3d) According to the single channel I–V relations measured under the different ionic conditions, the MS channel conductance for each ion at -100 mV was 42 pS (K⁺) 28 pS (Na⁺) 24 pS (Ba²⁺) and 13 pS (Ca²⁺). In all ionic conditions, there was evidence of some degree of inward rectification with conductance values measured at $+50$ of 15 pS (K⁺), ~ 10 pS (Na⁺), ~ 10 pS (Ba²⁺) and ~ 10 pS (Ca²⁺). The measurements with Na⁺ or K⁺ in Fig. 3c were made with zero Ca²⁺ and 5 mM EGTA in the pipette solution; when measurements were made with 1 mM Ca²⁺ (No EGTA) in the pipette solution the conductance values at -100 mV were reduced to 28 pS (K⁺) and 20 pS (Na⁺) (data not shown) consistent with Ca²⁺ permeant ion block of the MS cation channel (i.e., MscCa). These ion conductances are very similar to those measured for MscCa in *Xenopus* oocytes and human prostate tumor cells (Taglietti and Toselli 1988; Maroto et al. 2012).

In addition to the MS channel currents that were “spontaneously” active in approximately one third of mESC patches, another much larger unitary current was detected at much lower frequency in cell-attached patches (2 out of 165). Figure 4 shows recordings from one patch of a ~ 10 pA inward currents at -50 mV with 100 mM K⁺ in the pipette (under the same conditions MscCa was ~ 1.5 pA) which reversed at ~ 0 mV and at 70 mV became large outward currents that displayed relaxations after channel opening and

closing (Fig. 4 top trace). Similar relaxations associated with large conductance Ca²⁺-activated K⁺ (BK_{Ca2+}) channels have been reported in small chromaffin cells and interpreted as evidence that the single channel current is sufficient to discharge/recharge the cell’s membrane capacitance/membrane potential (Fenwick et al. 1982). In our case, the current relaxations indicate that at least some mESCs exhibit a very high resting membrane resistance, similar to small chromaffin cells. The low probability of occurrence of the large K⁺ currents in mESC patches may indicate low functional expression and/or low BK_{Ca2+} channel activity due to, for example, a low resting [Ca²⁺]_i (i.e., <0.2 μ M). However, because BK_{Ca2+} channels can also be activated by strong depolarization without [Ca²⁺]_i elevation (Barrett et al. 1982; Hille 2001) we also routinely examined activity at depolarized patch potentials (>50 mV)—again no increased evidence of BK channel activity was detected in over 100 patches. In contrast, and as described below, a similar depolarization of cell-attached patches on human ESCs revealed large outward currents in >50 % of the patches studied.

Inside-Out Patch Recordings from Mouse Embryonic Stem Cells

In order to directly test for Ca²⁺-activated channels in mESCs, we recorded activity from inside-out patches with

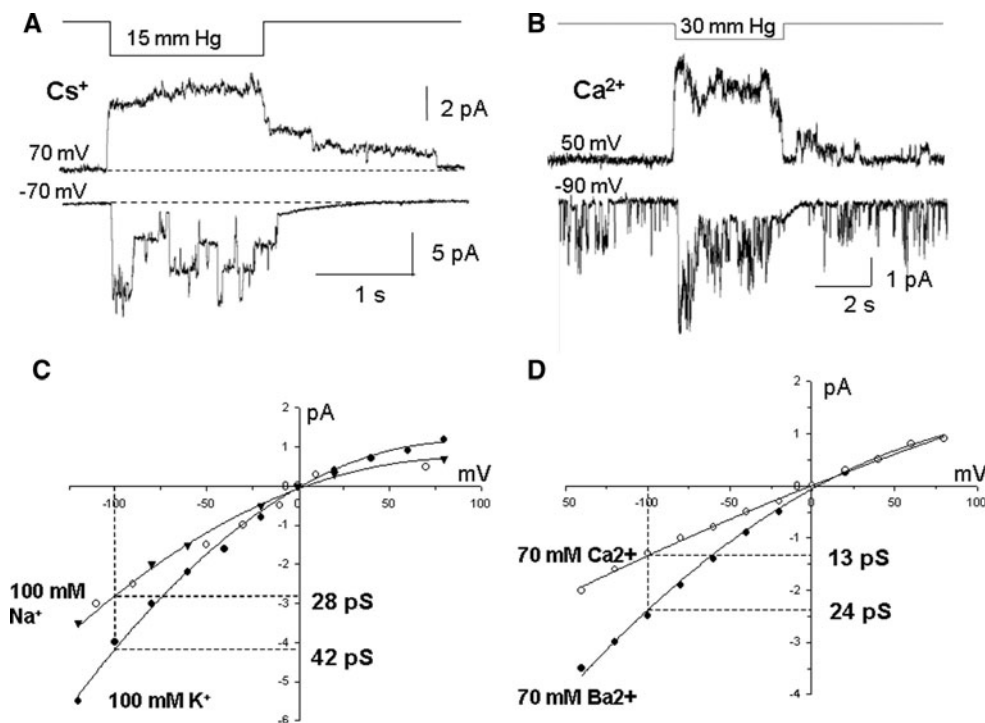


Fig. 3 Cell-attached patch recordings from mESCs illustrating MS channel conductance properties. **a** MS currents evoked by 15 mmHg suction pulses applied to the patch held at ± 70 mV patch potentials with the 100 mM Cs⁺/5 mM EGTA pipette solution. **b** MS currents evoked on a different patch from another cell held at -90 and 50 mV with a 70 mM Ca²⁺ pipette solution. **c** Current–voltage (I–V) relations of single MS channel currents measured with pipette

solutions of 100 mM Na⁺/5 mM EGTA and 100 mM K⁺/5 mM EGTA. **d** I–V relations measured with 70 mM Ca²⁺ and 70 mM Ba²⁺ pipette solutions. The data points and lines were fitted to pass through the origin in order to facilitate visual comparison of relative inward conductance of Na⁺ versus K⁺ and Ba²⁺ versus Ca²⁺ (each I–V was based on data points from 2 to 3 patches)

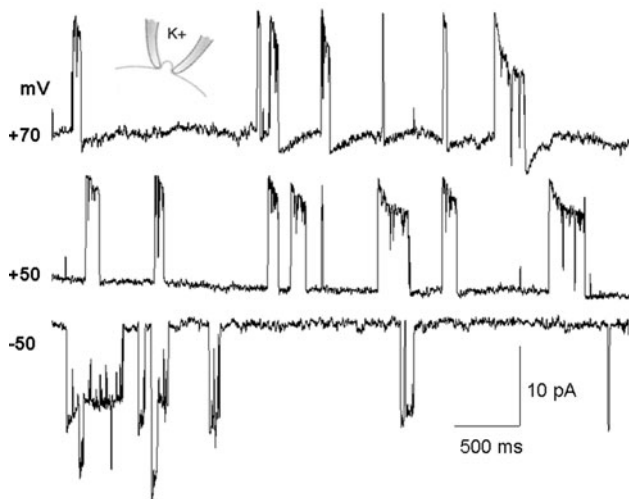


Fig. 4 A cell-attached patch recording from a mouse ESC showing large amplitude unitary inward and outward currents displaying relaxations immediately after channel opening and closing. The current traces were recorded with a 100 mM K⁺/5 mM EGTA pipette solution at the indicated patch potentials

the internal/cytoplasmic membrane face exposed to 1 mM Ca²⁺. Recordings from 32 out of 43 inside-out patches indicated the presence of additional high channel activity.

However, rather than large unitary K⁺ currents, the activity indicated a smaller (~ 25 pS) nonselective cation channel (NSCC). Figure 5a displays the typical protocol used in forming the inside-out patch configuration on mESCs—after initial tight seal formation and a brief period of baseline cell-attached recording (Fig. 5a, top current trace), the pipette tip was pulled away from the cell and then quickly passed through the solution/air interface (Fig. 5a, bottom trace). This procedure typically led to the rapid appearance of a sustained, high frequency occurrence of inward unitary current events of 1–2 pA, and on top of this background activity suction pulses activated MS current events. However, not all patches expressed both types of activities. For example, the cell-attached patches (30 %) that did not express MS currents also showed no MS channel activity in the inside-out patch configuration, although >50 % of these mechanoinsensitive patches did express the sustained activity with patch excision. Figure 5b (top two traces) illustrates this sustained channel activity that reversed at ~ 0 mV and displayed no evidence of voltage-dependent activation/inactivation (range ± 70 mV) or stretch-dependent activation/inactivation (Fig. 5b, bottom current trace). In still other inside-out patches, it was possible to record MS currents in the

absence of the sustained channel activity (Fig. 5c) indicating that the two activities are likely mediated by spatially distinct channel molecules. Furthermore, the two channels displayed distinguishable I–V relations (Fig. 5d) with an inward rectifying MS channel (32 pS –100 mV and 10 pS at 100 mV) and ohmic (nonrectifying) 25 pS channel (Fig. 5d). However, the 25 pS channel like the MS channel is also a nonselective cation channel (NSCC) that conducts Na⁺, K⁺ (Fig. 6A1) Cs⁺ (Fig. 6A2) and the divalents Ba²⁺ (Fig. 6B1) and Ca²⁺ (Fig. 6B2). Interestingly, high external Ca²⁺ (70 mM) reduced NSCC opening frequency (Fig. 6B2, see –70 mV trace) which was in contrast to the increase high Ca²⁺ caused in the spontaneous openings of MS channels (Fig. 3b, see –90 mV trace). Previous studies indicate a variety of NSCCs in different cell types with conductance values of 20–30 pS but with different Ca²⁺ sensitivities (Nilius et al. 1993; Guinamard et al. 2012). In mESCs, we found that the NSCC activity was only partially reduced when Ca²⁺ at the inside membrane face was reduced from 1 mM to a nominally Ca²⁺-free solution (Fig. 6c).

In summary, of the 43 inside-out patches excised from mouse ESCs, 24 expressed both MscCa and NSCC, 4 expressed only NSCC, 6 expressed only MscCa, and 9 patches failed to express any activity. Because none of the inside-out patches expressed BK_{Ca2+} channel activity, we can conclude that this channel has very low functional expression in mESCs.

Cell-Attached Patch Recordings from Human Embryonic Stem Cells

To test whether human ESCs express a similar channel profile as mESCs we recorded from the hESC line, HS181. A total of 68 cell-attached patches were studied, 51 of which were also studied in the inside-out patch configuration. In contrast to mESC patches, we observed MS channels in only 2 out of the 68 hESC patches (~3 %) using suction pulses approaching the near rupture suction (i.e., ~100 mm Hg). The amplitude and stretch sensitivity of the MS channels in the two hESC patches appeared similar to that measured in mESCs (Fig. 7a) but a more detailed comparison of the channel's conductance/ion selectivity properties was not possible. Another major difference between mouse and human ESCs patch recordings was the relatively high frequency occurrence of a BK channel current which was seen in >50 % of the cell-attached patches recorded at depolarized potentials. Figure 7b shows a recording, initially at resting and hyperpolarized potentials (–30, –60, and –90 mV) and then stepped to a more depolarized potential of +30 mV (Fig. 7B1), which revealed large (~12 pA) outward unitary currents (Fig. 7B2). In a few cell-attached patches

(~20 %) large amplitude inward currents were also recorded at negative potentials (Fig. 7c) allowing I–V relations to be measured over a full voltage range and indicated a single channel conductance of ~200 pS (Fig. 7d). The high spontaneous activity may indicate an elevated internal [Ca²⁺] in these cells. Interestingly, none of the BK channel currents in hESC cell-attached patches showed relaxations as seen for BK channels in mESCs (cf. Figs. 4, 7b, c) indicating a relatively lower resting membrane resistance for hESCs.

Inside-Out Patch Recordings from Human Embryonic Stem Cells

Inside-out patches excised from hESCs into normal Krebs' solution revealed two distinct channel activities—the most obvious was seen with 100 mM K⁺ in the pipette solution and involved large inward currents at resting and hyperpolarized potentials (Fig. 8a) that were clearly Ca²⁺ sensitive because switching the bath solution to a nominally Ca²⁺-free solution reversibly abolished their activity (Fig. 8b). The channel was also highly K⁺ selective because inward current could not be detected with Cs⁺ or Na⁺ at the external membrane face (data not shown), and outward currents could not be detected with Na⁺ at the internal membrane face (Fig. 6A1). The other channel activity seen on hESCs inside-out patches was similar in conductance to the NSCC described above. However, in hESC patches the NSCC inward current activity was only obvious in patches that did not express BK channels (Fig. 8c) or when recording at negative potentials with 100 mM Na⁺ (or 100 mM Cs⁺) in the pipette solution (data not shown). Overall, at least 30 % of inside-out patches from hESCs showed evidence of the NSCC activity.

Comparison of Mouse and Human ESC Patch Channel Profiles

Figure 9 shows pie charts that summarize the channel profiles for the three types of channels recorded in mESCs and hESCs. Whereas mESCs patches express most commonly MscCa, then NSCC and only rarely BK channels, hESCs patches express most commonly the BK_{Ca2+} channel, less obviously the NSCC, and very rarely MscCa. Mouse ESCs had 70 % MscCa active patches with an average density of 5 channels/patch and an overall average density of 3.5 channels/patch for all patches. Human ESCs had 3 % active patches with 1 channel/patch, the overall average density of only ~0.03 channel/patch. As discussed below these values can be converted to functional membrane channel density assuming a typical patch has an area of ~10 μm² for typical measured C_m values of ~0.1 pF (Sakmann and Neher 1983).

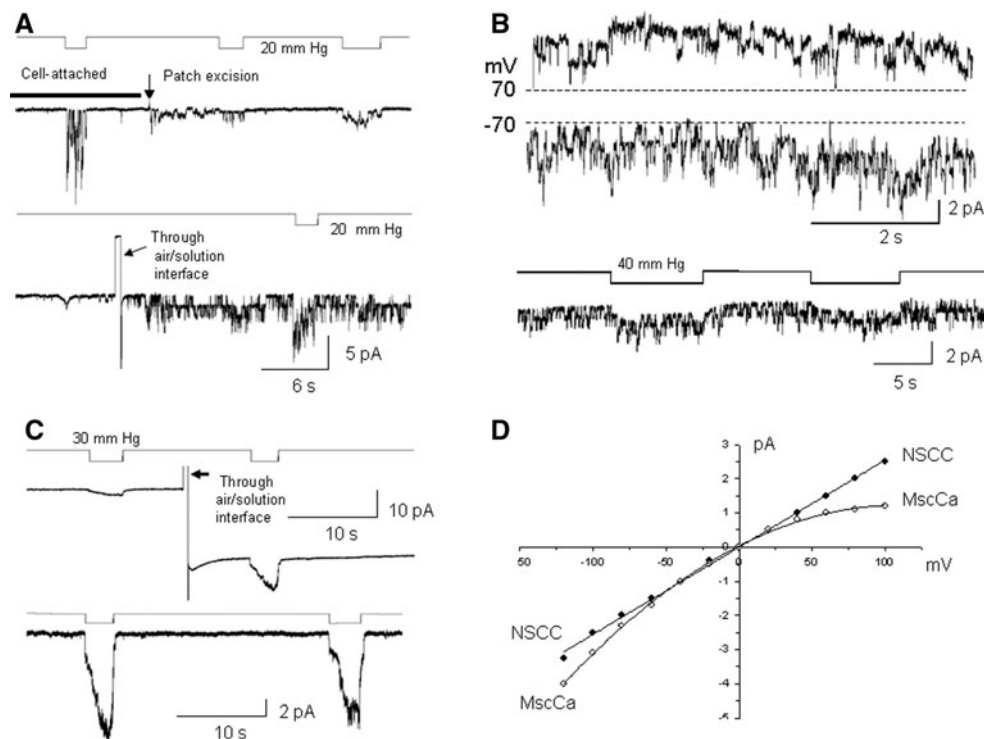


Fig. 5 Inside-out patch formation and recordings from mouse ESCs. **a** Sequence of steps carried out in inside-out patch formation from a mESC. The upper current trace shows an initial period of cell-attached recording (during solid line) in which MS currents activated by a 20 mmHg suction pulse. At the arrow, the pipette was withdrawn from the cell that induced an initial brief, noisy burst of current that was followed by MS unitary currents that were smaller than recorded cell-attached (i.e., consistent with removal of the driving force of the cell's membrane potential). The lower current trace was recorded ~1 min after patch excision, during which the pipette tip was rapidly passed through the solution-air interface (causing a large current artifact) and this induced the appearance of high frequency unitary inward current activity consistent with 2–3 channel openings. Application of suction pulses to the cell-free patch induced an additional MS current on top of this activity. The recording was made with a patch solution of 100 K⁺/5 EGTA at a patch potential of -80 mV with the inside face of the patch exposed to standard mammalian solution. **b** Upper two traces show recording from another inside-out mESC patch in which outward (at 70 mV) and inward (-70 mV) current activity was recorded with a pipette solution of 100 K⁺/5 EGTA and standard mammalian bathing solution. The lower trace shows recording from the same patch at

-70 mV during application of suction pulses were applied. Although this stimulation caused a shift in the current level it did so without increasing unitary current frequency; presumably the shift arises from suction-induced, reversible change in the seal resistance/leak current. **c** Another inside-out patch that expressed MS channel activity but not the high frequency current activity seen in patches described in **a** and **b**. In this case, after patch excision the pipette tip was passed through the air-solution interface increasing the amplitude of the MS current (i.e., consistent vesicle rupture and inside-out patch formation). However, the large, robust MS currents occurred in the absence of the background sustained activity. The pipette solution was 100 K⁺/5 EGTA recorded at a patch potential of -100 mV and isolated in the standard mammalian bathing solution. **d** Current-voltage relations of the MS and background unitary currents measured in inside-out patches excised from mESCs with a pipette solution of 100 K⁺/5 EGTA and isolated in standard mammalian solution. Both currents reversed at ~0 mV, and the curves were fitted to pass through the origin to facilitate comparison of the I-V relations. Whereas the I-V for the MS currents displayed inward rectification the background current displayed a linear I-V over the same voltage range with a single channel conductance of 25 pS

Discussion

Using single channel patch clamp recording we have identified three types of gated membrane ion channels in mouse and human ESCs—MscCa, BK_{Ca2+} and NSCC. We will focus here mainly on MscCa because of the recent intense interest in the role of mechanosensitive signaling pathways in regulating ESC biology (Discher et al. 2009; Cohen and Chen 2008; Keung et al. 2010; D'Angelo et al. 2011; Lee et al. 2011; Sun et al. 2012). Our results indicate that MscCa is expressed in both ESCs, but with much

higher frequency in mESC patches. In contrast, we found no evidence of MscK in ESCs of either species. Previous transcriptional analyses of ESCs have reported the expression of a variety of voltage-gated K⁺ channel proteins (Wang et al. 2005; Ng et al. 2010; Jiang et al. 2010) but so far there have been no reports of the expression patterns of two-pore domain K⁺ channel subunits that form MscK (Patel et al. 2001; Brohawn et al. 2012). In the case of MscCa, our results indicate an inwardly rectifying, nonselective cation channel that undergoes Ca²⁺ permeant block, shows voltage-dependent open channel lifetime,

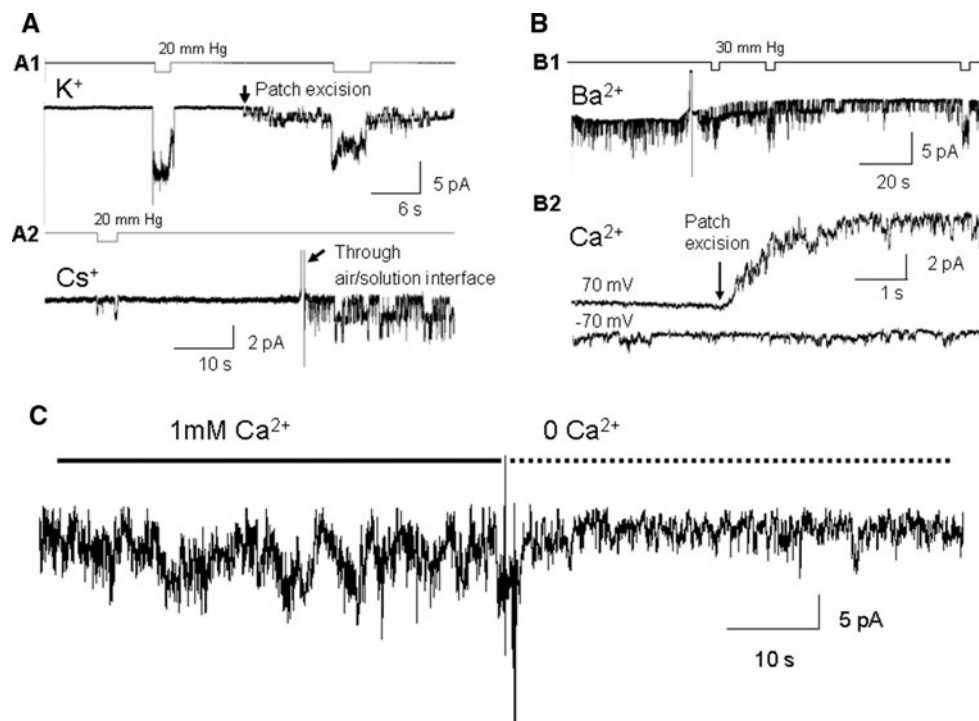


Fig. 6 Conductance properties and Ca²⁺ sensitivity of sustained channel activity measured in inside-out mESC patches. **a** Inward channel currents measured with either K⁺ or Cs⁺ as the predominant cation in the pipette solution. **A1** Initial cell-attached recording indicated no background current activity but a robust MS current in response to a suction pulse. Withdrawal of the pipette from the cell resulted in the immediate appearance of a unitary inward current activity (i.e., in this case solution-air interface penetration was not carried out) and a significant MS current. Pipette solution was 100 mM K⁺/5 mM EGTA and the excised patch potential was -50 mV. **A2** Similar to **A1** except the pipette solution was 100 Cs⁺/5

EGTA, and the patch potential was -70 mV. **b** Ba²⁺ and Ca²⁺ permeate the background channel activated on inside-out patches from mESCs. **B1** Inside-out patch formed with 70 mM Ba²⁺ in the pipette solution shows high frequency background unitary inward current activity. **B2** Inside-out patch with 70 mM Ca²⁺ pipette solution. **c** The Ca²⁺ sensitivity of the background inward current activity recorded from an inside-out patch from a mESC. After patch excision and “air exposure” a noisy background inward current was induced and this current was reduced but not abolished by perfusion of the inside membrane face with Krebs solution without added Ca²⁺ (i.e., nominally Ca²⁺-free)

stimulus-induced channel adaptation/inactivation, and multiple conductance state behavior. Similar channel features have been reported for the MscCa endogenously expressed in other cell types, including frog oocytes and human prostate tumor cells (Taglietti and Toselli 1988; Hamill and McBride 1992; Wu et al. 1998; Gil et al. 2001; Maroto et al. 2012). Indeed, when recorded under the same ionic conditions, the I–V relations of MscCa in the 3 cell types can be superimposed (cf. I–Vs in Fig. 3c with fig. 3C of Taglietti and Toselli 1988, and fig. 9B of Maroto et al. 2012). This indicates that closely related proteins most likely form the channels in the different cell types. To date, several candidate proteins have been proposed, including specific members of transient receptor potential (TRP) subfamilies (e.g., TRPC, TRPM, and TRPV). However, either their direct stretch sensitivity (TRPC1, TRPC6) has not proven reproducible (Maroto et al. 2005, 2012; Spassova et al. 2006; Gottlieb et al. 2008) and/or as homomeric channels (TRPC1, TRPV4, TRPM7) they do not express the same single channel properties (i.e.,

conductance, rectification, and/or divalent sensitivity) as the endogenous MscCa (Numata et al. 2007; Loukin et al. 2010; Ma et al. 2011; Chokshi et al. 2012; Zanou et al. 2009; Ho et al. 2012; Vasquez et al. 2012). On the other hand, a much stronger case has been made for members of the Piezo/Fam38 protein family. In particular Piezo1—identified from a Neuro2A cell cDNA library by Piezo1-siRNA’s selective blockade of the endogenous whole cell MS current—shares many of the MscCa properties (e.g., stretch sensitivity, conductance, ion selectivity, and pharmacology). Interestingly, the closely related Piezo2 also expresses a MS channel, but with distinctly different inactivation kinetics. In this case, it will be interesting to determine if the two Piezos are coexpressed in ESCs, and if different Piezo oligomers underlie the multiple conductance states of MscCa. For the nicotinic-, glycine-, and GABA-receptor channels that display similar multiple conductance state behavior as MscCa (Hamill and Sakmann 1981; Hamill et al. 1983) it has been shown that different oligomeric proteins produce different

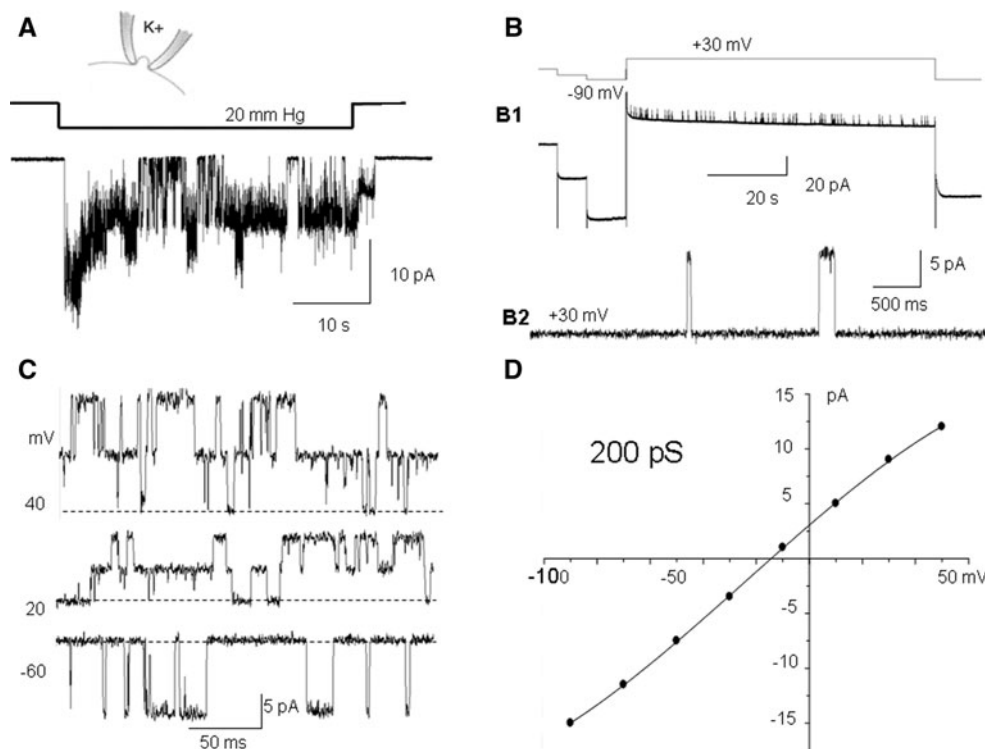


Fig. 7 Cell-attached recordings from human ESCs showing MS inward channel currents and BK channel activity. **a** Patch recordings of MS channel activity. Pipette solution was 100 mM K⁺/5 mM EGTA and the patch potential was -120 mV. **b** *Upper trace (B1)* show patch current during step changes in patch potential. Initial recordings were at the resting and hyperpolarized potentials (-30 , -60 , and -90 mV) and no unitary currents were detected. However,

when the patch was depolarized to $+30$ mV, outward unitary current activity was evident. *Lower trace (B2)* a higher gain trace showing the large nonrelaxing outward currents (~ 11 pA) recorded at $+30$ mV. The pipette solution was 100 K⁺/5 EGTA. **c** Voltage dependence of spontaneous large unitary currents recorded at the indicated patch potentials from a hESC cell-attached patch. **d** I-V plots of the currents shown in **c**. Pipette solution was 100 mM K⁺/5 mM EGTA

conductance states (Mishina et al. 1986; Bormann et al. 1993). On the other hand, transitions between conductance substates may occur because individual subunits within the multimeric membrane protein can switch between conformations resulting in partial channel opening (Gil et al. 2001; Vasquez et al. 2012). A different but not mutually exclusive mechanism involves the cytoplasmic “gondola” domain (i.e., hanging below the transmembrane pore domain) that by undergoing reorganization due to protein–protein interactions may also modulate ion permeation through the pore (Tierney 2011). The latter mechanism is attractive because a variety of channels, including the bacterial MS multistate channels, possess prominent gondolas (Steinbacher et al. 2007). Furthermore, it could explain the ability of cytoplasmic proteins (e.g., dystrophin) to modulate the stretch-sensitive transitions in the skeletal muscle MscCa (Vasquez et al. 2012).

In terms of functional expression, MscCa shows a higher patch density in mouse ESCs (i.e., 70 % active patches with an overall average density of ~ 3.5 channels/patch) compared with human ESCs (i.e., 3 % active patches with an overall density of ~ 0.03 channels/patch). On the basis of these estimates, one would predict that if the whole cell

membrane could be stretched to open all the MS channels (e.g., by expanding an elastic substrate) then the MS currents would be ~ 50 pA/pF for mESCs and ~ 0.5 pA/pF for hESCs (based on $i \sim 1.5$ pA at -50 mV and assuming a patch of $\sim 10 \mu\text{m}^2$ for C_m values of ~ 0.1 pF; Sakmann and Neher 1983). Furthermore, assuming ~ 20 % of the MscCa single channel current is carried by Ca²⁺ (see Zou et al. 2004) then the corresponding stretch-activated Ca²⁺ current would be ~ 10 pA/pF for mESC and ~ 0.1 pA/pF for hESC. To put these numbers in perspective, a recent whole cell patch clamp study of T-Type Ca²⁺ current in several different mouse ESC lines (including the D3 cell line studied here) measured an average Ca²⁺ current of ~ 5 pA/pF at 20 mV (Rodríguez-Gómez et al. 2012). Furthermore, the same study reported that blocking the T-Type Ca²⁺ channel with Ni²⁺ reduced mESC self renewal and pluripotency. At this time there is no information on the relative expression and function of T-type Ca²⁺ currents in human ESCs.

If stretch-activated Ca²⁺ influx plays a strictly house keeping function in ESCs and/or is essential for unique ESC functions (i.e., unlimited self renewal and pluripotency) then MscCa should be expressed at comparable

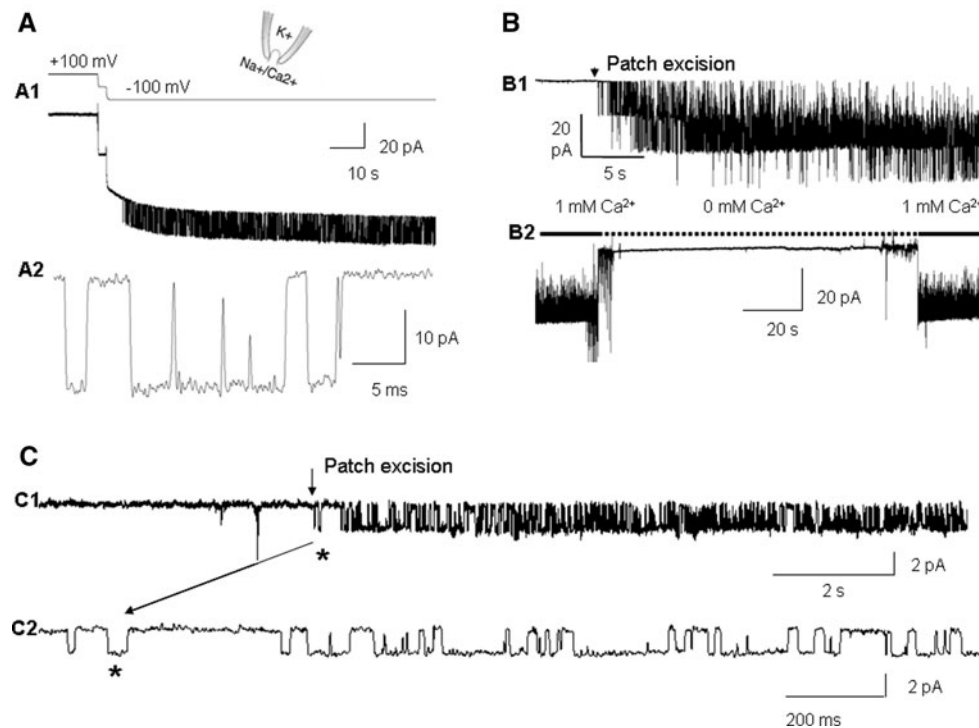


Fig. 8 Recordings of large unitary inward K⁺ channel (BK) currents and NSCC currents from inside-out patches isolated from human ESCs. **a** Inside-out patch isolated in normal mammalian solution (Na⁺/Ca²⁺). *Top trace (A1)* shows the absence of unitary currents at +100 and 0 mV but with hyperpolarization to -100 mV a high frequency of unitary inward currents of ~20 pA were evident consistent with a K⁺ selective channel. The *lower trace (A2)* shows higher resolution recordings of the single channel inward currents. The patch pipette solution was 100 mM K⁺/5 mM EGTA and the internal face of the inside out patch was exposed to normal mammalian bathing solution. **b** Ca²⁺ sensitivity of the large inward

K⁺ channel currents. Patch recording immediately after patch excision (*upper trace*) shows high frequency inward currents consistent with the simultaneous opening of three BK channels. *Lower trace in b* is a continuation of the patch recording ~1 min later, showing that replacement of the external Krebs's solution (i.e., containing 1 mM Ca²⁺) with a nominally Ca²⁺- free solution, resulted in a rapid block of the inward current activity (during *dashed line*) that recovered with return to the 1 mM Ca²⁺ Krebs's solution. **c** Inside-out patch recording from a human ESC that expressed a small inward current and not the BK current. Pipette solution 100 mM K⁺ 5 EGTA

levels in both mouse and human ESCs. That this is not the case favors the alternative explanation that MscCa activity underlies the different growth and differentiation requirements of mouse and human ESCs. In particular, it has been shown that the two ESCs require different types of mechanical interactions with their surrounding cells and their extracellular matrix, both for their survival and maintained pluripotency (Ginis et al. 2004; Sato et al. 2003; Hayashi et al. 2007; Chowdhury et al. 2010; Xu et al. 2010). Furthermore, cyclic stretch protocols applied to the cells can produce opposing effects on their fate decisions. For example, in the case of mESC lines (including the D3 cell line) the most consistent effect of cyclic stretch is to promote mESC differentiation into cardiovascular cell lineages (Schmelter et al. 2006; Gwak et al. 2008; Shimizu et al. 2008; Heo and Lee 2011; Wan et al. 2011; but see Horiuchi et al. 2012). In contrast, in a study of two different human ESC lines, cyclic stretch inhibited spontaneous ESC differentiation and promoted pluripotency (Saha et al. 2006, 2008; but see Teramura et al. 2012).

Although some variations, both within and between species, may reflect differences in the stretch protocols used (e.g., the cyclic strain frequencies ranged from 10 to 60 cycles/min over durations from 1 h to 14 days) it is notable that when mESCs and hESCs were both exposed to 14 days of cyclic stretch, opposing effects on pluripotency and differentiation were observed (Saha et al. 2006; Gwak et al. 2008). An intriguing correlate that may relate to the different responses has been reported in proliferating ESC colonies where human ESCs undergo a higher rate of spontaneous differentiation at the center of the cell colony, whereas mouse ESCs are more likely to differentiate at the colony edges (Oh et al. 2005; Johnson et al. 2008). Because cellular strain that develops within a growing 3-D embryoid body is not be uniform, and should be lowest at the colony center where the cell layers are thickest and highest at the edge where the cells are thinnest, these opposite responses are consistent with the apparent different responses to applied cycle strain. Significantly, different signaling pathways have also been implicated in underlying

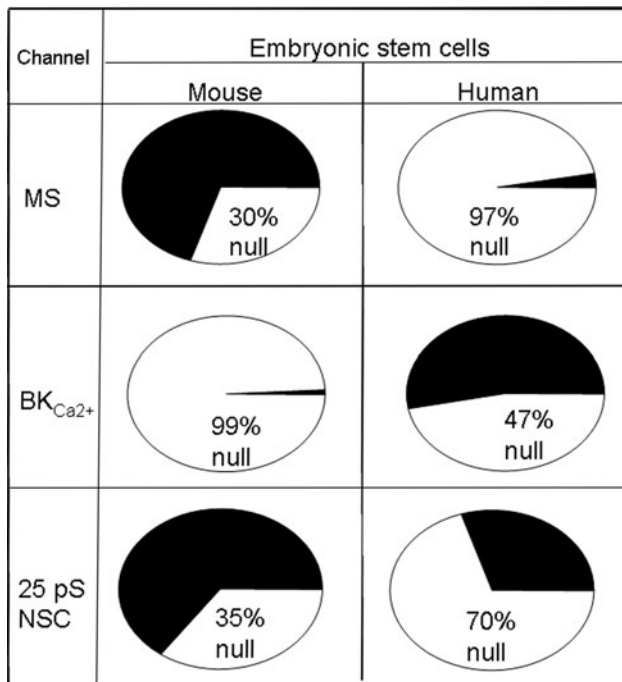


Fig. 9 The relative proportion of patches on mouse and human ESCs that express specific classes of channel currents, namely, MS cation channels, $\text{BK}_{\text{Ca}^{2+}}$ channels and nonselective 25 pS cation channels. The pie chart for the mouse ESCs is based on results from 185 cell-attached patches (43 of which were also recorded in inside-out configuration). Out of the 185, 130 patches (70 %) expressed MS channels, 28 out of 43 inside-out patches (65 %) expressed the 25 pS cation channel and evidence of the BK channel was seen in only 2 cell-attached patches (1 %) recorded at depolarized potentials and in none of the zero inside-out patches. In the case of human ESCs, of the 68 cell-attached patches studied only 2 displayed MS channels (3 %), 36 out of 68 displayed BK channel activity (53 %) at depolarized potentials, and at least 15 out of 51 inside-out patches (30 %) showed evidence of the 25 pS cation channel

the different responses. In the case of the strain-induced inhibition of hESC differentiation, it has been proposed that stretch-induced release of transforming growth factor-beta ($\text{TGF-}\beta$) ligands and activation of $\text{TGF-}\alpha$ /Activin/Nodal signaling produce the inhibition of differentiation and the maintenance of pluripotency (Saha et al. 2008). In the case of mESCs, stretch-induced generation of ROS and integrin-mediated PI3K-Akt signaling appears to promote differentiation (Schmelter et al. 2006; Heo and Lee 2011). It is also known that force applied to integrins can activate MS channels (Hayakawa et al. 2007) and Ca^{2+} influx via MscCa can increase ROS generation via (Ammar et al. 2005). Moreover, MscCa activity is itself stimulated by ROS generation (Khairallah et al. 2012). In this case, the stretch-induced response of mouse ESCs may reflect a relatively exaggerated stretch-induced Ca^{2+} influx due to higher MscCa expression. On the other hand, in human mESCs the predominate effect of cyclic stretch may be to elevate constitutive membrane trafficking and secretion, which has

been shown to occur independent of MscCa activation (Maroto and Hamill 2001). Future experiments involving suppression/up-regulation of MscCa expression in ESCs, and testing responses to cyclic strain protocols, should prove useful in testing these ideas.

The other class of channel we found expressed in ESCs is the large conductance K^{+} selective (BK) channel, which was detected at higher frequency in hESC patches (53 %) compared with mESC patches (~ 1 %). Furthermore, using inside-out patches isolated from hESCs it was possible to directly demonstrate that BK channels were highly Ca^{2+} sensitive (i.e., $\text{BK}_{\text{Ca}^{2+}}$ channels). Assuming an average BK channel density of ~ 1 channel/patch for hESCs and ~ 0.01 channel/patch for mESCs, the whole cell maximal BK currents (i.e., activated by elevated $[\text{Ca}^{2+}]_i$ and/or depolarization) would be ~ 100 pA/pF for hESCs and ~ 1 pA/pF for mESCs at 40 mV (i.e., based on a single BK channel current of 10 pA at 40 mV). To add perspective to these estimates, previous whole cell patch recordings indicated depolarization-activated outward K^{+} currents (IK) of 47.5 pA/pF for hESCs and 8.6 pA/pF for mESCs when stepped to 40 mV (Wang et al. 2005). Moreover, in the same study it was demonstrated that inhibition of the whole cell K^{+} current by TEA or the specific $\text{BK}_{\text{Ca}^{2+}}$ channel blocker, iberiotoxin (IBTX), also inhibited ESC proliferation (Wang et al. 2005). The role of $\text{BK}_{\text{Ca}^{2+}}$ channel in regulating cell proliferation has also been indicated by studies of other cell types in which overexpression or activation of BK channels was shown to promote proliferation (Ouadid-Ahidouch et al. 2004; Bloch et al. 2007; Coiret et al. 2007) whereas blocking BK channels inhibited proliferation (Basrai et al. 2002). Moreover, a study of breast cancer cells found that IBTX only inhibited cell proliferation when $[\text{Ca}^{2+}]_i$ was elevated by ATP pulses, and not when $[\text{Ca}^{2+}]_i$ remained at basal levels (Roger et al. 2004). Because both mouse and human ESCs express ATP, histamine or dopamine receptors that promote Ca^{2+} release from IP3 sensitive stores (Yanagida et al. 2004; Apati et al. 2012) a differential $\text{BK}_{\text{Ca}^{2+}}$ channel expression could mean that even with similar receptor densities/activations and elevations in $[\text{Ca}^{2+}]_i$, the accompanying membrane hyperpolarization, increased Ca^{2+} driving force and activation of downstream signaling pathways could be quite different in human and mouse ESCs.

The third class of single channel current identified in ESCs was a 25 pS nonselective cation channel (NSCC) activated upon inside-out patch formation but which was neither stretch activated nor strongly $[\text{Ca}^{2+}]_i$ dependent. This presumably indicates that other cytoplasmic factors normally suppress its activity on cell-attached patches. Previous reports indicate similar ~ 25 pS NSCC activated on inside-out patches from a variety of cell types but the

protein identity and exact mechanism of activation of these channels has yet to be defined (Koivisto et al. 1998; Large 2002; Guinamard et al. 2012). Given that activation of NSCC would tend to depolarize the cell and counter the effect of any K⁺ channel activation, then NSCC could play a key role in regulating ESC fate decisions and/or subsequent differentiation. Although NSCC was seen more often in mESCs than in hESCs (~70 vs. 30 % of patches) the difference was not as dramatic as with MscCa and BK_{Ca2+} and its presence on some hESC patches may have been concealed by high BK channel activity.

In conclusion, our single channel patch clamp study adds to the list of membrane ion channels in ESCs that were previously identified using whole cell current measurements. In particular, several voltage-gated currents, including hyperpolarization-activated cation (HCN), depolarization-activated K⁺ (Kv), T-type Ca²⁺, and voltage-gated Na⁺ channels have been measured in one or both species of ESCs (Wang et al. 2005; Jiang et al. 2010; Kleger et al. 2010; Lau et al. 2011; Ng et al. 2010; Rodríguez-Gómez et al. 2012). In comparative studies, HCN currents were expressed in mESCs but not in hESCs, and larger (fivefold) Kv currents were recorded in hESC compared with mESC (Wang et al. 2005). Interestingly, human induced-pluripotent stem cells (hiPSC) also failed to express HCN currents but their Kv current density was more similar to that recorded in mESC than in hESC (Jiang et al. 2010). Regarding the homogeneity of channel expression in ESCs lines isolated from the same species, it has been shown that T-type Ca²⁺ and voltage-gated Na⁺ channel are expressed at comparable levels in four different mouse ESC lines (including D3) (Rodríguez-Gómez et al. 2012). On the other hand, a study of three different hESC lines found that each line displayed a unique expression signature (Abeyta et al. 2004) indicating that each hESC cell line may carry a unique version of the human genome that can be traced to the inner cell mass cells of a single embryo. In this case, it will be important to also compare channel expression signatures in different hESC lines, as well as in hiPSCs. Nevertheless, our patch clamp recordings, even though sampling a tiny fraction of the total membrane of mouse and human ESCs, indicate differences in the degree rather than in the kind of channel expression. In functional studies, in which Kv, HCN or T-type Ca²⁺ currents were genetically or pharmacologically blocked, the common finding was a binary rather than a graded response, with pluripotency/self-renewal inhibited and differentiation promoted. Similar studies targeting MscCa will be helpful in determining whether MscCa activity is permissive for the pluripotent or differentiated states.

Acknowledgments OH was supported by a travel/stay Grant from Ministerio de Educación y Ciencia (SAB2006-0211) and in the

United States by grants from the National Cancer Institute and the Department of Defense. BS and AH are supported by the Fundación Progreso y Salud, Consejería de Salud, Junta de Andalucía (PI-0022/2008); Consejería de Innovación Ciencia y Empresa, Junta de Andalucía (CTS-6505; INP-2011-1615-900000); FEDER cofunded grants from Instituto de Salud Carlos III (Red TerCel-RD06/0010/0025; PI10/00964), and the Ministry of Health and Consumer Affairs (Advanced Therapies Program TRA-120). CIBERDEM is an initiative of the Instituto de Salud Carlos III.

References

- Abeyta MJ, Clark AT, Rodriguez RT, Bodnar MS, Pera RA, Firpo MT (2004) Unique gene expression signatures of independently-derived human embryonic stem cell lines. *Hum Mol Genet* 13:601–608
- Amma H, Naruse K, Ishiguro N, Sokabe M (2005) Involvement of reactive oxygen species in cyclic stretch-induced NF- κ B activation in human fibroblast cells. *Br J Pharmacol* 145:364–373
- Apati A, Paszty K, Erdei Z, Szebenyl K, Homolya L, Sarkadi B (2012) Calcium signaling in pluripotent stem cells. *Mol Cell Endocrinol* 353:57–67
- Barrett JN, Magleby KL, Pallota BS (1982) Properties of single calcium-activated potassium channels in cultured rat muscle. *J Physiol* 331:211–230
- Basrai D, Kraft R, Bollensdor C, Liebmann L, Benndorf K, Patt S (2002) BK channel blockers inhibit potassium-induced proliferation of human astrocytoma cells. *NeuroReport* 3:403–407
- Bloch M, Ousingsawat J, Simon R, Schraml P, Gasser TC, Mihatsch MJ, Kunzelmann K, Bubendorf L (2007) KCNMA1 gene amplification promotes tumor cell proliferation in human prostate cancer. *Oncogene* 26:2525–2534
- Bormann J, Rundström N, Betz H, Langosch D (1993) Residues within transmembrane segment M2 determine chloride conductance of glycine receptor homo- and hetero-oligomers. *EMBO J* 12:3729–3737
- Brohawn SG, Del Marmol J, MacKinnon R (2012) Crystal structure of the human K2P TRAAK, a lipid- and mechano-sensitive K ion channel. *Science* 335:436–441
- Bronson SK, Smithies O (1994) Altering mice by homologous recombination using embryonic stem cells. *J Biol Chem* 269:27155–27158
- Cho H, Koo JY, Kim S, Park SP, Yang Y, Oh U (2006) A novel mechanosensitive channel identified in sensory neurons. *Eur J Neurosci* 23:2543–2550
- Chokshi R, Matsushita M, Kozak JA (2012) Sensitivity of TRPM7 channels to Mg²⁺ characterized in cell-free patches of Jurkat T lymphocytes. *Am J Physiol* 302:C1642–C1651
- Chowdhury F, Li Y, Poh YC, Yokohama-Tamaki T, Wang N, Tanaka TS (2010) Soft substrates promote homogeneous self-renewal of embryonic stem cells via down regulating cell-matrix tractions. *PLoS ONE* 5(12):e15655
- Cohen DM, Chen CS (2008) Mechanical control of stem cell differentiation. In: *StemBook*. Harvard Stem Cell Institute, Cambridge, MA
- Coiret G, Borowiec AS, Mariot P, Ouaïd-Ahidouch H, Matifat F (2007) The antiestrogen tamoxifen activates BK channels and stimulates proliferation of MCF-7 breast cancer cells. *Mol Pharmacol* 71:843–851
- Coste B, Mathur J, Schmidt M, Earley TJ, Ranade S, Petrus MJ, Dubin AE, Patapoutian A (2010) Piezo1 and Piezo2 are essential components of distinct mechanically activated cation channels. *Science* 330:55–60

- D'Angelo F, Tiribuzi R, Armentano I, Kenny JM, Martino S, Orlacchio A (2011) Mechanotransduction: tuning stem cells fate. *J Funct Biomater* 2:67–87
- Danciu TE, Adam RM, Naruse K, Freeman MR, Hauschka PV (2003) Calcium regulates the PI3K–Akt pathway in stretched osteoblasts. *FEBS Lett* 536:193–197
- Discher DE, Mooney DJ, Zandstra PW (2009) Growth factors, matrices, and forces combine and control stem cells. *Science* 324:1673–1677
- Dreesen O, Brivanlou AH (2007) Signaling pathways in cancer and embryonic stem cells. *Stem Cell Rev* 3:7–17
- Evans M, Kaufman M (1981) Establishment in culture of pluripotent cells from mouse embryos. *Nature* 292:154–156
- Fenwick EM, Marty A, Neher E (1982) A patch-clamp study of bovine chromaffin cells and of their sensitivity to acetylcholine. *J Physiol* 331:577–597
- Gil Z, Magleby K, Silberberg SD (2001) Two-dimensional kinetic analysis suggests nonsequential gating of mechanosensitive channels in *Xenopus* oocytes. *Biophys J* 81:2082–2099
- Ginis I, Luo Y, Miura T, Thies S, Brandenberger R, Gerecht-Nir S, Amit M, Hoke A, Carpenter MK, Itskovitz-Eldor J, Rao MS (2004) Differences between human and mouse embryonic stem cells. *Dev Biol* 269:360–380
- Gottlieb PA, Sachs F (2012) Piezo1: properties of a cation selective mechanical channel. *Channels* 6:214–219
- Gottlieb P, Folgering J, Maroto R, Raso A, Wood TG, Kurosky A, Bowman C, Bichet D, Patel A, Sachs F, Martinac B, Hamill OP, Honoré E (2008) Revisiting TRPC1 and TRPC6 mechanosensitivity. *Pflugers Arch* 455:1097–1103
- Guinamard R, Paulais M, Lourdel S, Teulon J (2012) A calcium-permeable non-selective cation channel in the thick ascending limb apical membrane of the mouse kidney. *Biochim Biophys Acta* 1818:1135–1141
- Gwak SJ, Bhang SH, Kim IK, Kim SS, Cho SW, Jeon O, Yoo KJ, Putnam AJ, Kim BS (2008) The effect of cyclic strain on embryonic stem cell-derived cardiomyocytes. *Biomaterials* 29:844–856
- Hamill OP (2006) Patch clamp technique. *Encyclopedia of life science*. Wiley, New York
- Hamill OP, Martinac B (2001) Molecular basis of mechanotransduction in living cells. *Physiol Rev* 81:685–740
- Hamill OP, McBride DW Jr (1992) Rapid adaptation of the mechanosensitive channel in *Xenopus* oocytes. *Proc Natl Acad Sci USA* 89:7462–7466
- Hamill OP, Sakmann B (1981) Multiple conductance states of single acetylcholine receptor channels in embryonic muscle cells. *Nature* 294:462–464
- Hamill OP, Marty A, Neher E, Sakmann B, Sigworth F (1981) Improved patch clamp techniques for high current resolution from cells and cell-free membrane patches. *Pflugers Arch* 391:85–100
- Hamill OP, Bormann J, Sakmann B (1983) Glycine and GABA active multiple conductance state chloride channels in spinal cord neurones. *Nature* 305:805–808
- Hayakawa K, Tatsumi H, Sokabe M (2007) Actin stress fibers transmit and focus force to activate mechanosensitive channels. *J Cell Sci* 121:496–503
- Hayashi Y, Furue KM, Okamoto T, Ohnuma K, Myoshi Y, Fukuhara Y, Abe T, Satao JD, Hata RI, Asashima M (2007) Integrins regulate mouse embryonic stem cell self-renewal. *Stem Cells* 25:3005–3015
- Heo JS, Lee JC (2011) β -Catenin mediates cyclic strain-stimulated cardiomyogenesis in mouse embryonic stem cells through ROS-dependent and integrin-mediated PI3K/Akt pathways. *J Cell Biochem* 112:1880–1889
- Hille B (2001) Ion channels of excitable membranes, 3rd edn. Sinauer Associates, Sunderland
- Hmadcha A, Domínguez-Bendala J, Wakeman J, Arredouani M, Soria B (2009) The immune boundaries for stem cell based therapies: problems and prospective solutions. *J Cell Mol Med* 13:1464–1475
- Ho TC, Horn NA, Huynh T, Kelava L, Lansman JB (2012) Evidence TRPV4 contributes to mechanosensitive ion channels in mouse skeletal muscle fibers. *Channels* 6:246–254
- Horiuchi R, Akimoto T, Hong Z, Ushida T (2012) Cyclic mechanical strain maintains Nanog expression through PI3K/Akt signaling in mouse embryonic stem cells. *Exp Cell Res* 318:1726–1732
- Hovatta O, Mikkola M, Gertow K, Stromberg AM, Inzunza J, Hreinsson J, Rozell B, Blennow E, Andang M, Ahrlund-Richter L (2003) A culture system using human foreskin fibroblasts as feeder cells allows production of human embryonic stem cells. *Hum Reprod* 18:1404–1409
- Jiang P, Rushing SN, Kong CW, Fu J, Lieu DK, Chan CW, Deng W, Li RA (2010) Electrophysiological properties of human induced pluripotent stem cells. *Am J Physiol* 289:C486–C495
- Johnson BV, Shindo N, Rathjen PD, Rathjen J, Keough RA (2008) Understanding pluripotency—how ESC keep their options open. *Mol Hum Reprod* 4:513–520
- Kapur N, Mignery GA, Banach K (2007) Cell cycle dependent calcium oscillations in mouse embryonic stem cells. *Am J Physiol* 292:C1510–C1518
- Keung AJ, Kumar S, Schaffer DV (2010) Presentation counts: microenvironmental regulation of stem cells by biophysical and material cues. *Annu Rev Cell Dev Biol* 26:533–556
- Khairallah RJ, Shi G, Sbrana F, Prosser BL, Borroto C, Mazaitis MJ, Hoffman EP, Mahurkar A, Sachs F, Sun Y, Chen YW, Raiteri R, Lederer WJ, Dorsey SJ, Ward CW (2012) Microtubules underlie dysfunction in duchenne muscular dystrophy. *Sci Signal* 5(236):ra56
- Kleger A, Seufferlein T, Malan D, Tischerdorf M, Storch A, Wolhein A, Latz S, Protze S, Porzner M, Proepper C, Brunner C, Katz SF, Varma Pusapati G, Bullinger L, Franz WM, Koehntop R, Giehl K, Spyranis A, Wittekindt O, Lin Q, Zenke M, Fleischmann BK, Warthenberg M, Wobus AM, Boeckers TM, Liebau S (2010) Modulation of calcium-activated potassium channels induces cardiogenesis of pluripotent stem cells and enrichment of pacemaker-like cells. *Circulation* 122:1823–1836
- Koestenbauer S, Zech NH, Juch H, Vanderzwalmen P, Schoonjans L, Dohr G (2006) Embryonic stem cells: similarities and differences between human and murine embryonic stem cells. *Am J Reprod Immunol* 55:169–180
- Koivisto A, Klinge A, Nedergaard J, Siemen D (1998) Regulation of the activity of 27 pS nonselective cation channels in excised membrane patches from rat brown-fat cells. *Cell Physiol Biochem* 8:231–245
- Kung C (2005) A possible unifying principle for mechanosensation. *Nature* 436:647–654
- Large WA (2002) Receptor-operated Ca²⁺-permeable nonselective cation channels in vascular smooth muscle: a physiologic perspective. *J Cardiovasc Electrophysiol* 13:493–501
- Lau YT, Wong CK, Luo J, Leung LH, Tsang PF, Bian ZX, Tsang SY (2011) Effects of hyperpolarization-activated cyclic nucleotide-gated (HCN) channel blockers on the proliferation and cell cycle progression of embryonic stem cells. *Pflugers Arch* 461:191–202
- Lee DA, Knight MM, Campbell JJ, Bader DL (2011) Stem cell mechanobiology. *J Cell Biochem* 112:1–9
- Loukin S, Zhou XL, Su ZW, Saimi Y, Kung C (2010) Wild-type and brachyolmia-causing mutant TRPV4 channels respond directly to stretch force. *J Biol Chem* 285:27176–27181

- Ma X, Nilius B, Wong JW, Huang Y, Yao X (2011) Electrophysiological properties of heteromeric TRPV4-C1 channels. *Biochim Biophys Acta* 1808:2789–2797
- Machaca K (2010) Ca²⁺ signaling, genes and the cell cycle. *Cell Calcium* 48:243–250
- Maroto R, Hamill OP (2001) Brefeldin A block of integrin-dependent mechanosensitive ATP release from *Xenopus* oocytes reveals a novel mechanism of mechanotransduction. *J Biol Chem* 276:23867–23872
- Maroto R, Raso A, Wood TG, Kurosky A, Martinac B, Hamill OP (2005) TRPC1 forms the stretch-activated cation channel in vertebrate cells. *Nat Cell Biol* 7:1443–1446
- Maroto R, Kurosky A, Hamill OP (2012) Mechanosensitive Ca²⁺ permeant channels in human prostate tumor cells. *Channels* 6:290–307
- Martin G (1981) Isolation of a pluripotent cell line from early mouse embryos cultured in medium conditioned by tetracarcinoma stem cells. *Proc Natl Acad Sci USA* 78:7634–7638
- Martinac B (2012) Mechanosensitive ion channels: an evolutionary and scientific tour de force in mechanobiology. *Channels* 6:211–213
- Mishina M, Takai T, Imoto K, Noda M, Takahashi T, Numa S, Methfessel C, Sakmann B (1986) Molecular distinction between fetal and adult forms of muscle acetylcholine receptor. *Nature* 321:406–411
- Naruse K, Yamada T, Sokabe M (1998) Involvement of SA channels in orienting response of cultured endothelial cells to cyclic stretch. *Am J Physiol* 274:H1532–H1538
- Ng SY, Chin CH, Lau YT, Luo J, Wong CK, Bian ZX, Tsang SY (2010) Role of voltage-gated potassium channels in the fate determination of embryonic stem cells. *J Cell Physiol* 224:165–177
- Nilius B, Droogmans G, Gericke M, Schwarz G (1993) Nonselective ion pathways in human endothelial cells. *EXS* 66:269–280
- Numata T, Shimizu T, Okada Y (2007) TRPM7 is a stretch- and swelling-activated cation channel involved in volume regulation in human epithelial cells. *Am J Physiol* 292:C460–C467
- Oh SK, Kim HS, Park YB, Seol HW, Kim YY, Cho MS, Ku SY, Choi YM, Kim DW, Moon SY (2005) Methods for expansion of human embryonic stem cells. *Stem Cells* 23:605–609
- Ostrow LW, Suchyna TM, Sachs F (2011) Stretch induced endothelin-1 secretion by adult rat astrocytes involves calcium influx via stretch-activated ion channels (SACs). *Biochem Biophys Res Commun* 410:81–86
- Ouadid-Ahidouch H, Roudbaraki M, Ahidouch A, Delcourt P, Prevarskaya N (2004) Cell-cycle-dependent expression of the large Ca²⁺-activated K⁺ channels in breast cancer cells. *Biochem Biophys Res Commun* 316:244–251
- Patel AJ, Lazdunski M, Honoré E (2001) Lipid and mechano-gated 2P domain K⁺ channels. *Curr Opin Cell Biol* 3:422–428
- Pease S, Williams RL (1990) Formation of germ-line chimeras from embryonic stem cells maintained with recombinant leukemia inhibitory factor. *Exp Cell Res* 190:209–211
- Pera MF, Tam PPL (2010) Extrinsic regulation of pluripotent stem cells. *Nature* 465:713–720
- Rao M (2004) Conserved and divergent paths that regulate self renewal in mouse and human embryonic stem cells. *Dev Biol* 275:269–286
- Rodríguez-Gómez JA, Levitsky KL, López-Barneo J (2012) T-type Ca²⁺ channels in mouse embryonic stem cells: modulation during cell cycle and contribution to self-renewal. *Am J Physiol* 302:C494–C504
- Roger S, Potier M, Vandier C, Le Guennec JY, Besson P (2004) Description and role in proliferation of iberiotoxin-sensitive currents in different human mammary epithelial normal and cancerous cells. *Biochim Biophys Acta* 1667:190–199
- Saha S, Juan LJ, De Pablo JJ, Palecek SP (2006) Inhibition of human embryonic stem cell differentiation by mechanical strain. *J Cell Physiol* 206:126–137
- Saha S, Juan LJ, De Pablo JJ, Palecek SP (2008) TGFβ/Activin/Nodal pathway in inhibition of hESC differentiation by mechanical strain. *Biophys J* 94:4123–4133
- Sakmann B, Neher E (1983) Geometric parameters of pipettes and membrane patches. In: Sakmann B, Neher E (eds) *Single-channel recording*. Plenum Press, New York, pp 37–76
- Sato N, Sanjuan IM, Heke M, Uchida M, Naef F, Brivanlou AH (2003) Molecular signature of human embryonic stem cells and its comparison with the mouse. *Dev Biol* 260:404–413
- Schmelter M, Ateghang B, Helmig S, Watenberg M, Sauer H (2006) Embryonic stem cells utilize reactive oxygen species as transducers of mechanical strain-induced cardiovascular differentiation. *FASEB J* 20:E294–E306
- Schwirtlich M, Emri Z, Antal K, Mate Z, Katarova Z, Szabo G (2010) GABA(A) and GABA(B) receptors of distinct properties affect oppositely the proliferation of mouse embryonic stem cells through synergistic elevation of intracellular Ca²⁺. *FASEB J* 24:1218–1228
- Shimizu N, Yamamoto K, Obi S, Kumagaya S, Masumura T, Shimano Y, Naruse K, Yamashita JK, Igarashi T, Ando J (2008) Cyclic strain induces mouse embryonic stem cell differentiation into vascular smooth muscle cells by activating PDGF receptor. *J Appl Physiol* 104:766–772
- Smith AG (2001) Embryo-derived stem cells: of mice and men. *Annu Rev Cell Dev Biol* 17:435–462
- Spasova MA, Hewavitharana T, Xu W, Soboloff J, Gill DL (2006) A common mechanism underlies stretch activation and receptor activation of TRPC6 channels. *Proc Natl Acad Sci USA* 103:16586–16591
- Steinbacher S, Bass R, Strop P, Rees DC (2007) Structures of the prokaryotic mechanosensitive channels MscL and MscS. *Curr Top Membr* 58:1–24
- Suchyna TM, Besch SR, Sachs F (2004) Dynamic regulation of mechanosensitive channels: capacitance used to monitor patch tension in real time. *Phys Biol* 1:1–18
- Sun Y, Chen CS, Fu J (2012) Forcing stem cells to behave: a biophysical perspective of the cellular microenvironment. *Annu Rev Biophys* 41:519–542
- Sundelacruz S, Levin M, Kaplan DL (2009) Role of membrane potential in the regulation of cell proliferation and differentiation. *Stem Cell Rev Rep* 5:231–246
- Taglietti V, Toselli M (1988) A study of stretch-activated channels in the membrane of frog oocytes: interactions with Ca²⁺ ions. *J Physiol* 407:311–328
- Teramura T, Takehara T, Onodera Y, Nakagaw K, Hamanishi C, Fukuda K (2012) Mechanical stimulation of cyclic tensile strain induces reduction of pluripotent related gene expressions via activation of Rho/ROCK and subsequent decreasing of AKT phosphorylation in human induced pluripotent stem cells. *Biochem Biophys Res Commun* 417:836–841
- Thomas KR, Capecchi MR (1987) Site-directed mutagenesis by gene targeting in mouse embryo-derived stem cells. *Cell* 51:503–512
- Thomson JA, Itskovitz-Eldor J, Shapiro SS, Waknitz MA, Swiergiel JJ, Marshall VS, Jones JM (1998) Embryonic stem cell lines derived from human blastocysts. *Science* 282:1145–1147
- Tierney ML (2011) Insights into the biophysical properties of GABAA ion channels: modulation of ion permeation by drugs and protein interactions. *Biochim Biophys Acta* 1808:667–673
- Van Hoof D, Passier R, Ward-Van Oostwaard D, Pinkse MW, Heck AJ, Mummery CL, Krijgsveld J (2006) Quest for human and mouse embryonic stem cell-specific proteins. *Mol Cell Proteomics* 7:1261–1273

- Vasquez I, Tan N, Boonyasampant M, Koppitch KA, Lansman JB (2012) Partial opening and subconductance gating of mechanosensitive ion channels in dystrophic skeletal muscle. *J Physiol* 590:1–18
- Wan CR, Chung S, Kamm RD (2011) Differentiation of embryonic stem cells into cardiomyocytes in a compliant microfluidic system. *Ann Biomed Eng* 39:1840–1847
- Wang JG, Miyazu M, Matsushita E, Sokabe M, Naruse K (2001) Uniaxial cyclic stretch induces focal adhesion kinase (FAK) tyrosine phosphorylation followed by mitogen-activated protein kinase (MAPK) activation. *Biochem Biophys Res Comm* 288:356–361
- Wang K, Xue T, Tsang SY, Van Huizen R, Wong CW, Lai KW, Ye Z, Cheng L, Au KW, Zhang J, Li GR, Lau CP, Tse HF, Li RA (2005) Electrophysiological properties of human and mouse embryonic stem cells. *Stem Cells* 23:1526–1534
- Weissman I (2005) Stem cell research: paths to cancer therapies and regenerative medicine. *JAMA* 294:1359–1366
- Wu G, McBride DW Jr, Hamill OP (1998) Mg²⁺ block and inward rectification of mechanosensitive channels in *Xenopus* oocytes. *Pflugers Arch* 435:572–574
- Xu Y, Zhu Y, Hahm HS, Wei W, Hao E, Hayek A, Ding S (2010) Revealing a core signaling regulatory mechanism for pluripotent stem cell survival and self-renewal by small molecules. *Proc Natl Acad Sci USA* 107:8129–8134
- Yamamoto Y, Suzuki H (1996) Two types of stretch-activated channel activities in guinea-pig gastric smooth muscle cells. *Jpn J Physiol* 46:337–345
- Yanagida E, Shoji S, Hirayama Y, Yoshikawa F, Otsu K, Uematsu H, Hiraoka M, Furuichi T, Kawano S (2004) Functional expression of Ca²⁺ signaling pathways in mouse embryonic stem cells. *Cell Calcium* 36:135–146
- Yao X, Kwan H-Y, Huang Y (2001) Stretch-sensitive switching among different channels sublevels of an endothelial cation channel. *Biochim Biophys Acta* 1511:381–390
- Zanou N, Shapovalov G, Louis M, Tajeddine N, Gallo C, Van Schoor M, Anguish I, Cao ML, Schakman O, Dietrich A, Lebacqz J, Ruegg U, Roulet E, Birnbaumer L, Gailly P (2009) Role of TRPC1 channel in skeletal muscle function. *Am J Physiol Cell Physiol* 298:C149–C163
- Zou H, Lifshitz LM, Tuft RA, Fogarty KE, Singer JJ (2004) Imaging calcium entering the cytosol through a single opening of plasma membrane ion channels: SCCaFTs—fundamental calcium events. *Cell Calcium* 35:523–533